PHYSICAL REVIEW B **75**, 224434 (2007)

Magnetization dynamics induced by ultrashort optical pulses in Fe/Cr thin films

A. A. Rzhevsky
Institut für Festkörperforschung IFF-9 "Elektronische Eigenschaften," Forschungzentrum Jülich GmbH, D-52425 Jülich, Germany and Ioffe Physical Technical Institute, Russian Academy of Sciences, 194021 St. Petersburg, Russia

B. B. Krichevtsov
Ioffe Physical Technical Institute, Russian Academy of Sciences, 194021 St. Petersburg, Russia

D. E. Bürgler and C. M. Schneider
Institut für Festkörperforschung IFF-9 "Elektronische Eigenschaften," Forschungzentrum Jülich GmbH, D-52425 Jülich, Germany

(Received 11 February 2007; published 29 June 2007)

The magnetization dynamics of single-crystalline Fe(001) thin films with Cr cap layers has been studied by an all-optical time-resolved pump-probe technique. The system is characterized by a fourfold in-plane magnetic anisotropy. We observed long-lived (~1 ns) magnetization oscillations caused by the ultrafast (~0.15 ps) optical pulse excitation. The oscillations are associated with the temporal variation of the magnetization component M_z normal to the film surface. The phase of the oscillations is independent of the polarization state of the pump beam giving evidence for a predominantly thermal origin of the excitation. The amplitude of the oscillations considerably depends on the in-plane orientation and magnitude of the magnetic field. The azimuthal variation of the oscillation frequency at constant magnetic field follows the fourfold in-plane magnetic anisotropy. Angle and field variations of the frequency are well described by a uniform precession mode known from the theory of ferromagnetic resonance. Our analysis indicates that the precession amplitude is determined by the frequency of the uniform mode and an in-plane tilting of the effective magnetic field directly caused by the pumping light beam.

DOI: 10.1103/PhysRevB.75.224434 PACS number(s): 75.30.Gw, 76.50.+g, 78.20.Ls, 78.47.+p

I. INTRODUCTION

Magnetic thin films and multilayer structures offer the unique possibility to tailor magnetic and electrical properties of a system and to tune them over an extremely wide range. For this reason, these magnetic layer stacks are not only of general scientific interest but they also form major building blocks in spintronic devices used in information technology,[1,2] such as hard disk read heads, magnetic biosensors, magnetic random access memories, or magnetic logic. With respect to device functionality and performance, the issue of magnetic switching speed is currently in the focus of interest, driving a strong research activity in the fields of ultrafast spin and magnetization dynamics. It is known for some time that a short optical pulse may strongly affect the electronic structure of a metallic magnet due to the creation of a large number of hot electrons. The subsequent electronic deexcitation results in a "warming" of the spin and phonon subsystems, if one adopts a three-bath model.[3] This energy transfer to magnons and phonons can give rise to changes of the magnetization magnitude (quenching of ferromagnetic order), of the optical parameters of the film, and of the magnetic anisotropy parameters, causing specific optical, magnetic, and magneto-optical responses on short (<1.5 ps) and long (~1 ns) time scales.[3–13] On the short time scale, instantaneous changes of the reflected light intensity and a rotation of the polarization plane have been observed. These initial changes may be subsequently followed by an oscillatory response on a longer time scale, related to the excitation of long-lived precessional or acoustical modes.[14,15]

The phenomenon of laser pulse-induced persistent magnetization precession has been observed recently in polycrystalline nickel as well as in Permalloy ($Ni_{80}Fe_{20}$) films.[10,16] In these experiments, a specific initial state of **M** was defined by applying a magnetic field perpendicular to the film plane, i.e., turning the magnetization fully or partially out of the film plane and establishing a uniaxial configuration. The excitation of the magnetization precession in these experiments was related to the demagnetization and modification of the anisotropy by the optical pump pulse. In Ref. 12, real-space magnetization dynamics has been studied in Co and Ni films. It was experimentally proven that the ultrashort light pulse does not only result in a demagnetization but also triggers a fast (~1 ps) tilting of **M** away from the equilibrium direction, which is followed by a precession around the time-dependent effective magnetic field $\mathbf{H}_{eff}(t)$. On this time scale, $\mathbf{H}_{eff}(t)$ is determined by the rate of heat diffusion to the substrate, whereby this characteristic time may be even longer than the relaxation time of the precessional motion. A time-dependent contribution of the magneto-crystalline anisotropy to $\mathbf{H}_{eff}(t)$ was also demonstrated. The possibility to excite coherent magnetization dynamics in exchange-biased systems through ultrafast optical modulation of the exchange bias field—which is responsible for the unidirectional anisotropy—was explored in Ref. 17 and also studied in Refs. 18 and 19.

In general, the magnetization dynamics caused by a short intense light pulse is only incompletely described by the Landau-Lifshitz-Gilbert (LLG) equation, as the magnetization modulus as well as the value and direction of the effective field are becoming time-dependent functions during the relaxation processes.[12] Because of that, the spectrum, angle, and field dependencies of the magnetization precession fre-

quencies can be quite different from those observed in ferromagnetic resonance (FMR) or Brillouin light scattering (BLS). The role of the magnetic anisotropy in these dynamic processes, however, is still an open question, in particular, for nonuniaxial configurations. Therefore, it is interesting to compare the behavior of optically excited magnetization precession with LLG theory in systems, which are less anisotropic. One such example is a biaxially anisotropic Fe film grown on (100)-oriented substrates.

So far, various complementary techniques such as conventional and network analyzer FMR,[20–24] BLS,[25–28] and time-resolved magnetic-field pump-optical probe methods[29,30] have been used to access magnetic relaxation processes of anisotropic Fe, Fe_xCo_{1-x}, or Permalloy thin films grown on GaAs(100) substrates. In all of these experiments, the magnetization dynamics was driven by an external magnetic field, either in a sine-wave or pulsewise manner, the shortest pulse widths reaching down to about 10 ps. The excitation mechanisms of the magnetic system invoked by ultrashort (~100–200 fs) optical pulses differ inherently from those involved in the above-mentioned techniques. In contrast to standard FMR, the all-optical pump-probe method provides the possibility to investigate the free precession of **M** as well as to determine the frequency and damping parameters in a wide range of constant magnetic fields. Whereas BLS is dealing with thermal spin-wave excitations, the pump-probe method also provides the opportunity to study spin dynamics in a thermal nonequilibrium mode induced by the light pulse. In addition, the precessional motion and damping of the magnetization may be visualized in real time.

In this work, we employ an all-optical pump-probe method to investigate the influence of a fourfold in-plane magnetic anisotropy on the magnetization dynamics in thin magnetic monocrystalline Fe films. In contrast to previous all-optical studies of metallic systems, we have chosen a particular experimental geometry with the external magnetic field being applied in the plane of the film. This configuration allows us to investigate the amplitude, frequency, and damping of magnetization precession as a function of both orientation and magnitude of the in-plane magnetic field, as well as a function of the optical polarization configuration. In this context, we also note that the modification of the cubic magnetocrystalline anisotropy under ultrafast optical excitation has been studied recently in isolating ferromagnetic garnet films.[31] As a main result, the important role of nonthermal mechanisms caused by the excitation and manifesting themselves through a polarization-dependent magneto-optical response was demonstrated. The fourfold magnetic anisotropy along with the linear dichroism has also been exploited recently in the manipulation of magnetic states in magnetic semiconductors (Ga,Mn)As by ultrashort optical excitation.[32]

Thus, the goal of this paper is to investigate the magnetization dynamics in biaxially anisotropic Cr/Fe(100) thin films after excitation by ultrashort light pulses. We show that on the long time scale, the precessional motion of the magnetization is excited independent of the polarization of the pump beam. This finding gives evidence for a thermal mechanism being at work. The rotation of the probe beam

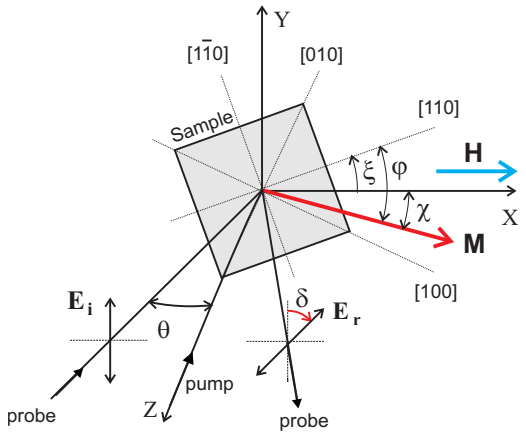

FIG. 1. (Color online) Geometry of the all-optical time-resolved pump-probe experiment. Here, X,Y,Z is a laboratory coordinate system; ξ, azimuthal angle of the hard axis; φ, angle between magnetization and hard axis; χ, azimuthal angle of the magnetization; θ, angle of incidence; and δ, angle of rotation of the polarization plane measured in the experiment.

polarization plane, i.e., the magneto-optic response, is caused by the oscillating magnetization component M_z perpendicular to the film surface. Frequency and amplitude of the precession mode strongly depend on the magnitude and orientation of the magnetic field and clearly reflect the fourfold in-plane magnetic anisotropy of the film. The results are in agreement with previously proposed mechanisms of optically induced magnetization dynamics, provided that effects due to the instantaneous demagnetization and change of the magnetocrystalline anisotropy are taken into account.

II. EXPERIMENTAL ASPECTS

The Fe (d=100 Å) films were grown on GaAs(001) substrates by molecular-beam epitaxy, with an Ag(1500 Å)/Fe(10 Å) buffer layer being deposited prior to the Fe film growth in order to provide better epitaxy.[33] The structure was covered by a Cr(10 Å) protective cap layer. The quality of the films has been monitored *in situ* by reflection high-energy electron diffraction (RHEED) during the growth process. After deposition the sample was removed from the chamber and fixed onto a sample holder allowing a 360° rotation around the surface normal. All measurements were performed at room temperature (T=294 K). The dynamic response of the magnetization **M** was induced by short (~150 fs) pump-light pulses (λ=800 nm, f=1 kHz) at normal incidence generated by a regenerative amplifier (SpitfirePro, SpectraPhysics). The geometry of the experiment and definitions of the angles are shown in Fig. 1. The diameter of the surface illuminated area was about 0.5 mm. The average pump power deposited into the surface was about 15 mW. The *s*-polarized probe beam was focused into a 50 μm diameter spot in the center of the area illuminated by the pump beam. The rotation of the polarization plane of the probe beam (δ) has been measured as a function of time delay Δt between pump and probe pulses. A polarization-sensitive differential photodetector and a lock-in technique

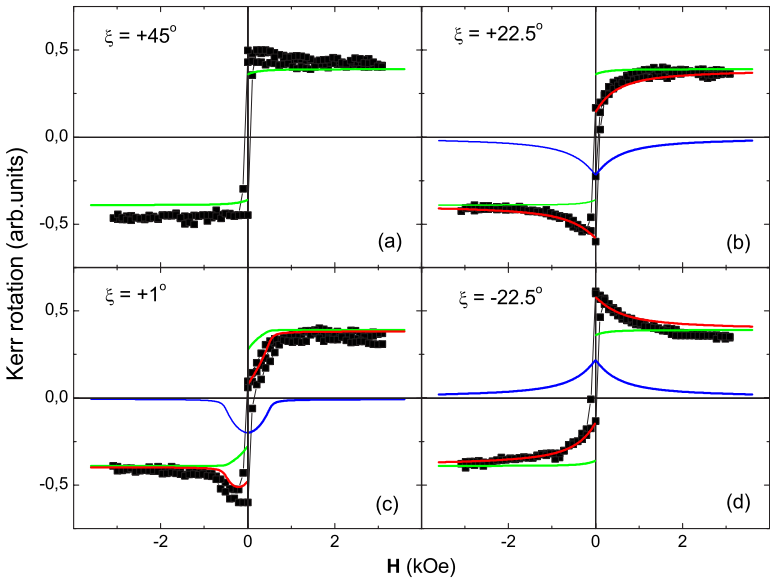

FIG. 2. (Color online) Longitudinal magneto-optical Kerr effect measured at $\lambda=800$ nm and an incidence angle $\theta=35°$ for different orientations of the in-plane magnetic field: (a) Magnetic field along the easy ([100]) axis, (b) and (d) magnetic field under an angle of $\xi=\pm 22.5°$ relative to the hard ([110]) axis, and (c) magnetic field oriented close to the hard axis. Solid lines are calculated contributions of linear ($\sim\mathbf{M}$, green) and quadratic ($\sim\mathbf{M}^2$, blue) terms. The total magneto-optical response is shown by red lines.

have been used to obtain a high sensitivity. The measurements have been carried out for two different probe beam incidence angles of $\theta=10°$ and $\theta\sim 35°$. The polarization state of the pump beam could be varied from linear to circular (left or right) by a corresponding rotation of a quarter wave plate. For comparison, the in-plane magnetic anisotropy of the films has also been studied employing the conventional longitudinal magneto-optical Kerr effect (see Fig. 2) using the same light source at the incidence angle of $\theta\sim 35°$.

III. QUASISTATIC MAGNETIZATION REVERSAL

A. Kerr effect observations

In the absence of a strong perpendicular magnetic field, the magnetization **M** of the films studied is oriented in plane, as the energy of the demagnetizing field $2\pi M_z^2$ by far exceeds the energy of the perpendicular uniaxial anisotropy $K_u M_z^2$, including both bulk and interfacial contributions. Therefore, we used the longitudinal magneto-optical Kerr effect (LMOKE) to characterize the quasistatic magnetization reversal in the films. In Figs. 2(a)–2(d), the LMOKE hysteresis loops measured for different orientations of the in-plane magnetic field **H** relative to the crystal axes are shown. The films display a clear in-plane fourfold magnetic anisotropy with an orientation of the easy axes and hard axes along [100]- and [110]-type crystallographic directions, respectively. The hysteresis loops for **H** parallel to the easy axis [Fig. 2(a)] exhibit a rectangular shape with a coercive field $H_c\sim 10$ Oe, indicating a reversal mechanism mainly based on domain-wall nucleation and motion. Along other directions, the magnetization reversal also involves significant rotation processes, as can be seen by the rounding of the loops after the initial jump at small fields [Figs. 2(b)–2(d)]. The magnetization rotation is completed at a saturation field of $H_s\sim 2.5$ kOe. The absolute magnitude of the Kerr rotation is about $\delta_{max}\sim 0.02°$ in the saturation region. When the magnetic field deviates from an easy or hard axis [Figs. 2(b) and 2(d)], we also see a clear asymmetry of the Kerr rotation loops, i.e., $\delta(H)\neq\delta(-H)$.

As an example, we take the loops measured at $\xi=\pm 22.5°$ [Figs. 2(b) and 2(d)]. Just after the initial jump at $H\sim 0$, the absolute value of the rotation of the polarization plane at $\xi=+22.5°$ [Fig. 2(b)] increases in positive and decreases in negative applied field. At $\xi=-22.5°$ [Fig. 2(d)], however, the magnitude of the longitudinal Kerr rotation decreases in positive and increases in negative applied magnetic field. The asymmetry character (of the $+22.5°$ or $-22.5°$ type) changes in a jumplike manner when the angle ξ between the magnetic field and the direction of the hard axis ([110]) changes sign. We also have to point out that a small angular deviation of the external field from the hard axis $\Delta\xi\sim 0.3°$ is sufficient for the asymmetry character to be changed. This is illustrated by Fig. 2(c). It corresponds to a case, in which the magnetic field is aligned very close (with an uncertainty of $\sim 1°$) with the hard axis. It is also interesting to note that in our LMOKE data, we do not find any indication for an in-plane uniaxial anisotropy. However, this finding is in agreement with the results of earlier FMR and BLS studies of ultrathin Fe films grown on Ag(100) substrates.[26,34]

B. Second-order contributions

The asymmetry of the longitudinal MOKE hysteresis loops shown in Fig. 2 is due to our choice of a rather steep angle of incidence θ and can be explained by taking into account higher-order contributions to the total magneto-optical response. In our case, this higher-order contribution is related to elements in the tensor of the dielectric susceptibility, which are second order or quadratic in the magnetization, i.e., $\sim\beta_{ijkl}M_k M_l$, and responsible for Cotton-Mouton (or Voigt) effect and magnetic linear dichroism.[35,36] These terms describe the *optical anisotropy* of the film induced by the magnetization **M**. For a thin film of cubic symmetry, one of the main directions of this optical anisotropy is parallel and the other is perpendicular to the direction of **M**. A rotation of

the magnetization is followed by a likewise rotation of the main optical anisotropy directions. This gives rise to a rotation of the polarization plane of the light, in addition to that induced by the linear Kerr effect. In contrast to the linear longitudinal magneto-optical Kerr effect, which is proportional to the magnetization component M_x lying in the incidence plane, the direction of the polarization plane rotation (clockwise or anticlockwise) caused by the quadratic in **M** terms is determined by the direction of the field-induced magnetization rotation. The latter is symmetric for positive and negative external fields at the same angle ξ. These quadratic contributions are responsible for the asymmetry observed in the hysteresis loops $\delta(H)$. For angles ξ of opposite sign, for example, $\xi=+22.5°$ and $\xi=-22.5°$, the rotation of the magnetization and the main directions of the optical anisotropy are also opposite. This manifests itself in an asymmetry of hysteresis loops for these angles.

Experimentally, the different contributions arising from the linear Kerr effect and from the quadratic response can be separated, if the sum and difference of the field dependencies $\delta(\mathbf{H})$ measured for opposite orientations ($\pm\xi$) of the in-plane magnetic field relative to a hard axis are taken, i.e., $O(\mathbf{M}) \sim \delta(\mathbf{H},+\xi)+\delta(\mathbf{H},-\xi)$ and $O(\mathbf{M}^2) \sim \delta(\mathbf{H},+\xi)-\delta(\mathbf{H},-\xi)$. The linear and quadratic in **M** contributions to the magneto-optical signal (rotation of the polarization plane) can also be calculated on the basis of the magnetic energy density ε. In this procedure, one needs to evaluate the angles $\chi=\xi-\varphi$, which determine the equilibrium orientation of the magnetization depending on the azimuthal orientation and magnitude of the applied field **H**. The task can be solved by means of a minimization of the magnetic energy potential. For bcc-Fe films grown on Ag(100), the following expression for ε has been shown to apply:[26,34]

$$\varepsilon(\varphi,\vartheta) = -HM_s\cos(\xi-\varphi)\sin\vartheta - \frac{K_1}{4}[\sin^4\vartheta\cos^2(2\varphi) + \sin^2(2\vartheta)] + 2\pi M_{eff}M_s\cos^2\vartheta, \quad (1)$$

where ϑ is the polar angle, describing the orientation of **M** relative to the surface normal, $4\pi M_{eff}=4\pi M_s-2K_\perp/M_s$, K_1 is the constant of the cubic in-plane magnetic anisotropy ($K_1<0$), and $K_\perp$ is the constant describing a surface-type perpendicular magnetic anisotropy. In Eq. (1), the first term describes the Zeeman contribution and the second one, the fourfold in-plane magnetic anisotropy energy. We neglect the in-plane uniaxial anisotropy term as well as the volume-type perpendicular uniaxial term, because they are considered to be small in the present case.[26,34] The minimization procedure leads to the solution of the transcendental equation

$$\sin(4\varphi) - A\sin(\xi-\varphi) = 0, \quad (2)$$

where $A=2HM/K_1$. Knowing the angle ξ, we can calculate the contribution to the rotation of the polarization plane in the longitudinal Kerr effect, which is defined by projection of the magnetization on x axis, i.e., $\delta(H)\sim\cos(\xi-\varphi)$. The contribution of quadratic in **M** terms $\beta(H)$ is proportional to M_xM_y, i.e., $\beta(H)\sim\sin(\xi-\varphi)\cos(\xi-\varphi)$. In order to obtain numerical results, we have chosen the following values for the magnetic parameters: $M_s=1.7$ kG, $4\pi M_s=2.1$ T, $2K_1/M_s=[0.55-2.5/d(\mathrm{ML})]$ kOe,[34] $K_\perp=0.5$ erg/cm,[2,25,26] and $d=100$ Å. The results of the calculation for the different contributions to the Kerr rotation are shown in Fig. 2 by solid lines. The good agreement between the experimental data and the calculated curves of the total magneto-optical signal proves the validity of the approach chosen. It should be noted that the contribution of quadratic terms to the total Kerr rotation is comparable in magnitude with the linear terms at least in small fields. Moreover, the magnetization rotation process is much more pronounced in $\beta(H)$ than in $\delta(H)$ dependencies.

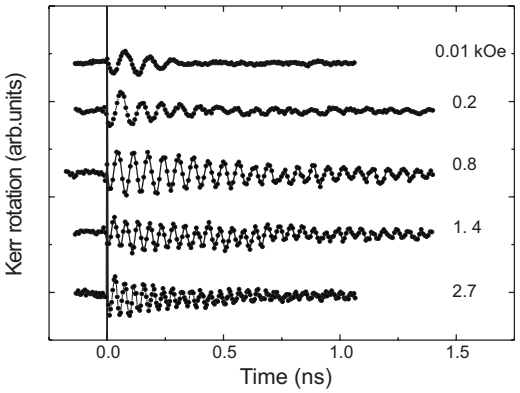

FIG. 3. Time profiles of the Kerr rotation for different values of the in-plane magnetic field as indicated. The field has been applied in between the easy and hard axes of the magnetization at $\xi=22.5°$.

IV. FAST MAGNETIZATION DYNAMICS

A. Excitation of precessional modes

In the experimental configuration that we have chosen, the excitation of the magnetic film system by the optical pump pulse manifests itself through an oscillatory magneto-optical response, i.e., an oscillatory rotation of the polarization plane of the probe beam. As we will discuss below, this time-resolved signal arises from the polar MOKE (PMOKE). Figure 3 displays the time profiles of this magneto-optical response for the experimental geometry with $\xi=22.5°$. Depending on the value of the external magnetic field **H**, we observe pronounced oscillations with different periodicities and damping characteristics. These oscillations obviously reflect the excitation of distinct precessional modes in the sample. Qualitatively, we can already note that an increase of the magnetic field appears to shift the frequency to higher values, whereas the behavior of the damping with the field strength seems to be more complicated. In order to arrive at a more quantitative interpretation, we extracted the main frequency components of the oscillations in time profiles like those in Fig. 3 using standard fast Fourier transformation procedures. In most cases, we found only one dominant frequency in the Fourier spectrum, which we will henceforth call resonance frequency. The damping characteristics are assumed to follow an exponential dependence (see Sec. V B).

The strong dependence of the frequency f of the oscillatory magneto-optical response on the magnitude and orienta-

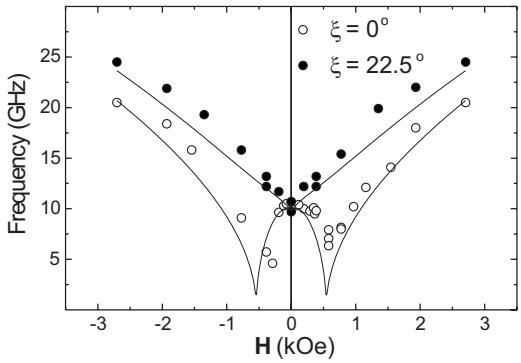

FIG. 4. Resonance frequency of the precessional modes as a function of the in-plane magnetic field measured in a Cr/Fe(001) film at two orientations of the in-plane magnetic field. The solid lines display the result of the calculations using Eq. (3).

tion of magnetic field (see Figs. 4 and 5) evidences that this oscillatory signal is related to the temporal variation of the magnetization **M** due to a precessional motion. This precessional motion also involves transient components of the magnetization perpendicular to the surface, i.e., $M_z(t)$. Thus, the experimentally observed magneto-optical rotation can be caused in principle by longitudinal and/or perpendicular magnetization components responsible for the longitudinal or polar Kerr effect, respectively, as well as by the presence of quadratic on M terms described above.

The measurements carried out at different incidence angles ($\theta=10°$ and 35°) of the probe beam, however, showed approximately the same amplitude for the oscillations. This allows us to eliminate effects due to the longitudinal component of **M**, i.e., a longitudinal MOKE contribution from further considerations. The amplitude of the oscillations depends only weakly on the polarization of the probe beam at $\theta=10°$. This finding is inconsistent with a mechanism involving effects due to $O(\mathbf{M}^2)$. Therefore, we can conclude that the oscillatory component of the magneto-optical signal is mainly caused by the temporal variation of M_z via the PMOKE. The polar Kerr effect is usually the largest among the magneto-optical effects in conducting magnetic films.[35] Using the value of the polar Kerr constant for bulk Fe, which is ~0.5° at $\lambda=800$ nm (Ref. 35) and taking into account that the maximal value of the oscillation amplitude is about

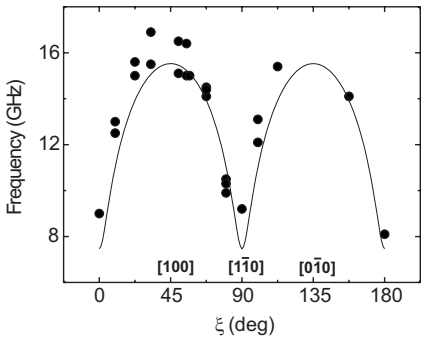

FIG. 5. Azimuthal variation of the precessional mode frequency at $H=0.8$ kOe. The solid line describes the result of the calculation using Eq. (3).

0.008° measured at $H=0.5$ kOe and $\xi=4°$, we arrive at a value of ~1° for the transient twisting angle of **M** away from the film plane.

B. Field and angular dependence of the dynamic Kerr response

We now turn to a more detailed analysis of the influence of the external field. In Fig. 4, the magnetic-field dependencies of the precession frequency are compiled for different orientations of the in-plane magnetic field $\xi=0°$ ($\mathbf{H}\|[110]$) and $\xi=22.5°$. We find that the absolute values of the resonance frequency and the shape of frequency variations depend quite strongly on the magnitude of the magnetic field and its orientation with respect to the anisotropy axes of the sample. For $\xi=0°$, the oscillation frequency varies from $f=4$ GHz at $H=0.3$ kOe up to $f=20$ GHz at $H=2.7$ kOe. For $\xi=22.5°$, the variation of f lies in the interval from 9 to 25 GHz. We note that the magnetic-field dependence exhibits a distinct difference for the magnetic field pointing along the hard axis ($\xi=0°$) and in between the hard and easy axes ($\xi=22.5°$). In the latter case, the minimum frequency is found at zero external magnetic field, whereas in the first case, two minima appear at finite field values.

The presence of minima in the resonance frequencies when magnetizing a sample along the hard axis is well known from FMR and BLS studies.[28,34] It may be somewhat unexpected in our pulsed excitation measurements, because we cannot assume *a priori* that mainly the uniform magnetization precession mode will be excited. However, the result gives a suggestion that a more quantitative interpretation of our results may be possible on the basis of formalisms originally developed for resonance techniques, such as FMR. Following the arguments used in these formalisms, the minimum in the resonance frequency should be related to the vanishing of the effective field H_{eff} at certain external field values, because of the compensation of contributions from external and anisotropy fields [see Eq. (1)].

In Fig. 5, we show the azimuthal variation of the resonance frequencies for a constant value of the magnetic field ($H=0.8$ kOe) applied in the film plane. We clearly discern strongly anisotropic fourfold characteristics. However, it is important to note that the shape of the azimuthal variations cannot be described by a simple $\cos^2(2\varphi)$ function. Instead, broad maxima along [100] directions are followed by narrow minima along $[1\bar{1}0]$ directions. Detailed investigations also revealed that at constant azimuthal angle of the magnetic field, the phase of the oscillations did not change upon a magnetic-field reversal. At constant magnetic field, however, a change of sign of ξ ($\xi\rightarrow-\xi$) leads to a phase change of the precessional oscillations by 180°. The amplitude and the phase of the oscillations do not depend on the polarization state of the pump beam (linear or circular). They are also independent of the azimuthal orientation of the linear polarization of the pump beam with respect to the crystal axes.

We now have to explain the experimentally observed variations of the resonance frequency on the magnetic-field strength and orientation. Taking into account that the diameter of the pump beam was about ten times larger than the

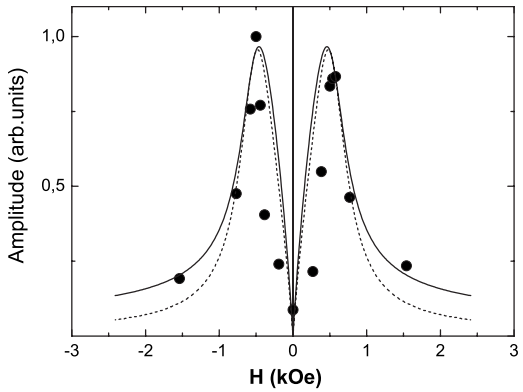

FIG. 6. Amplitude of the oscillations as a function of applied magnetic field **H** at constant azimuthal angle $\xi=4°$. The solid (dashed) line is the result of the calculation taking into account (neglecting) the frequency of the oscillations.

probe beam diameter and that we observed only one dominant frequency in most of our experiments, we assume that this frequency essentially marks the excitation of the uniform mode ($k=0$). Besides, we consider that the film is thin enough and that we can safely neglect any spatial variation of the magnetization over the film thickness. These approximations serve as input to a quantitative analysis of the time-resolved data, which will be based on a general formalism adapted from FMR theory. Within this formalism, the magnetic-resonance frequency f is defined by the following relationship:[37]

$$f=\frac{\gamma}{2\pi M_s \sin\vartheta}\sqrt{\frac{\partial^2\varepsilon}{\partial\varphi^2}\frac{\partial^2\varepsilon}{\partial\vartheta^2}-\left(\frac{\partial^2\varepsilon}{\partial\varphi\partial\vartheta}\right)^2}, \tag{3}$$

where $\gamma=ge/2mc$ is the gyromagnetic ratio, M_s is the saturation magnetization, and φ and ϑ are azimuthal and polar angles of the magnetization, respectively. $\varepsilon(\varphi,\vartheta)$ is the magnetic energy density described by Eq. (1).

The results of the calculations of f with the aid of Eq. (3) are presented by the solid lines in Figs. 4 and 5. The good agreement of the calculated curves with the experimental data supports our assumption that it is indeed mainly the uniform magnetization precession mode, which we measure in the center of the area illuminated by the pump beam.

V. PECULIARITIES OF THE OPTICAL EXCITATION

A. Limitations of the LLG approach

The amplitude of the oscillations strongly depends on both the orientation and magnitude of the in-plane magnetic field **H**. The most effective excitation of the precessional modes is observed, if the direction of the magnetic field is close to the hard axis and the magnitude of **H** is smaller than the saturation field H_s. As the magnetic-field direction approaches the easy axis, the amplitude of the oscillatory response decreases significantly. At magnetic fields larger than H_s, the oscillation amplitude also essentially decreases. In Fig. 6, we show the field dependence of the amplitude of the oscillations at $\xi=4°$. The dependence is characterized by a sharp maximum close to $H\approx 0.5$ kOe and a fast decrease at lower-field values. As the magnetic field increases above 0.5 kOe, the amplitude of the oscillations decreases more smoothly. We also note that at $\xi=22.5°$, the maximum value of the amplitude is smaller than at $\xi=4°$ and the peak is more washed out (not shown).

The excitation of the magnetization precession by the light pulse is caused by an ultrafast change of the direction of the effective field $\mathbf{H}_{eff}$. The pump pulse results in an instantaneous heating of the electron gas due to an avalanche excitation of the large number of hot electrons. After this initial step, due to electron-phonon and electron-magnon interactions, the electron gas energy is transferred to the phonon and magnon subsystems resulting in an increase of the respective temperatures. These processes take place on a time scale of $\tau_{e-e}\sim 0.1$ ps, $\tau_{e-ph}\sim 1.5$ ps, and $\tau_{e-sp}\sim 0.2$ ps,[14,38] correspondingly. As soon as thermal equilibration between these subsystems is achieved, a relatively slow decrease of the temperature inside the illuminated spot happens (τ_{therm} approximately nanosecond) due to heat diffusion from the illuminated area into the substrate and into the periphery of the film. The fast heating of the magnetic subsystem might be accompanied by a change of the magnitude of the magnetization by ΔM (Ref. 3) as well as a change of the magnetic anisotropy parameter by ΔK_1.[10–12,17] Prior to the pump pulse, the orientation of the magnetization **M** coincides with the direction of the effective magnetic field $\mathbf{H}_{eff}=-\partial\varepsilon/\partial\mathbf{M}$, where ε is the magnetic energy density [Eq. (1)]. The instantaneous change of the magnitudes of **M** and K_1 causes $\mathbf{H}_{eff}$ to rotate from the equilibrium position to the nonequilibrium configuration $\mathbf{H}^1_{eff}$. This process gives rise to the magnetization torque $\tau=[\mathbf{H}^1_{eff}\times\mathbf{M}]$ acting on magnetization **M**. If we do not take into account effects associated with a reduction of the modulus of the magnetic moment during the initial ultrafast excitation, the subsequent dynamic behavior of the magnetization should follow the Landau-Lifshitz-Gilbert equation

$$\frac{\partial\mathbf{M}}{\partial t}=-\gamma[\mathbf{M}\times\mathbf{H}^1_{eff}]+\frac{\alpha}{M_s}\left[\mathbf{M}\times\frac{\partial\mathbf{M}}{\partial t}\right], \tag{4}$$

where the second term describes the damping of the precessional motion of **M**. In a full dynamical approach, the modification of $|\mathbf{M}|$ by an ultrafast optical pulse leads to the appearance of additional terms in Eq. (4).[12] For the approximate treatment of the field and angular variations on the long time-scale magnetization precession amplitudes, however, we will consider their influence only as a perturbation to the magnetization movement described by Eq. (4).

The mechanism of the optically induced excitation of the precessional motion suggested in Ref. 10 assumes that after the absorption of the pump pulse, the effective field instantaneously changes its orientation $\mathbf{H}_{eff}\rightarrow\mathbf{H}^1_{eff}$, i.e., rotates by an angle $\Delta\psi$ for a short time τ and returns back to the initial state $\mathbf{H}^1_{eff}\rightarrow\mathbf{H}_{eff}$ almost as fast. For the time interval τ, the magnetization rotates around the new effective field direction $\mathbf{H}^1_{eff}$ and tilts away from the direction of $\mathbf{H}_{eff}$ by an angle $\phi\sim(\tau\omega)\Delta\psi$, where ω is the frequency of the uniform mode. After the effective field $\mathbf{H}^1_{eff}$ has relaxed back into the initial

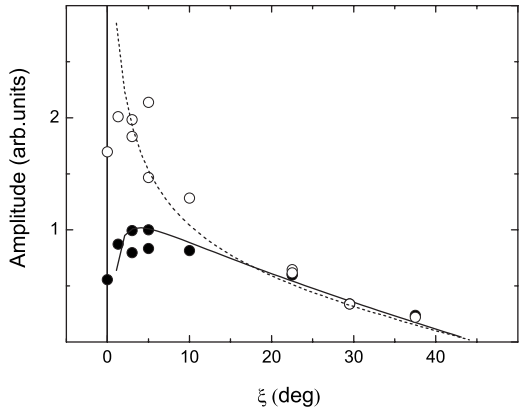

FIG. 7. Amplitude of the oscillations as a function of the azimuthal angle ξ at constant magnetic field $H=0.5$ kOe. Solid dots represent the experimental data; open dots mark the ratio between the experimentally measured amplitude of the oscillation and the oscillation frequency. Solid (broken) line: result of the model calculation taking into account (neglecting) the frequency of the oscillations.

state $\mathbf{H}_{eff}$, the magnetization continues to precess on an elliptical trajectory around the initial orientation of $\mathbf{H}_{eff}$, with the amplitude of the oscillations being proportional to $\omega\Delta\psi$.

The change $\Delta\psi$ of the direction of the effective field due to a possible demagnetization ΔM and a change of the anisotropy constant ΔK_1 can be estimated using Eq. (2), which determines the equilibrium orientation of the magnetization $\mathbf{M}$ at the given values of M and K_1. In an approximation, which takes only the terms linear in $\Delta M/M$ and $\Delta K_1/K_1$, it can be written as

$$\Delta\psi = \left(\frac{\Delta M}{M} - \frac{\Delta K_1}{K_1}\right) \Big/ [4\cot(4\varphi) - \cot(\xi - \varphi)]. \quad (5)$$

Using Eqs. (1) and (5) as well as the expression for the frequency of the uniform precession [Eq. (2)], we can finally calculate the shape of the field variations of $\Delta\psi$ and $\omega\Delta\psi$. The results are included in Fig. 6 as solid and dashed lines. The field variations of $\Delta\psi$ and $\omega\Delta\psi$ exhibit sharp maxima at $H\simeq 0.5$ kOe for a field orientation close to the hard axis ($\xi = 4°$). However, the decrease of $\omega\Delta\psi$ at $H>0.5$ kOe happens more slowly than for $\Delta\psi$. This difference is due to a strong dependence of the frequency ω on the magnitude of the external field. The frequency rises nearly linearly as the field increases beyond $H=0.5$ kOe (see Fig. 4).

The essential difference of $\Delta\psi$ and $\omega\Delta\psi$ is also visible in the azimuthal variations of the amplitude of the oscillations (Fig. 7). Again, the predictions of the calculations (solid and dotted lines) are in reasonable agreement with the experimental data points. We find that on approaching the hard axis ($\xi\to 0$), the magnitude of $\Delta\psi$ increases up to $\xi=0.3°$, while the magnitude of $\omega\Delta\psi$ and the experimentally measured amplitude of oscillation start to decrease at $\xi=4°$. This behavior is due to a fast decrease of the uniform mode frequency ω at $\xi\to 0$ (see Fig. 5). In Fig. 7, we also show the ratio between the experimental value of the oscillation amplitude and the oscillation frequency by open dots. It is seen that the ratio

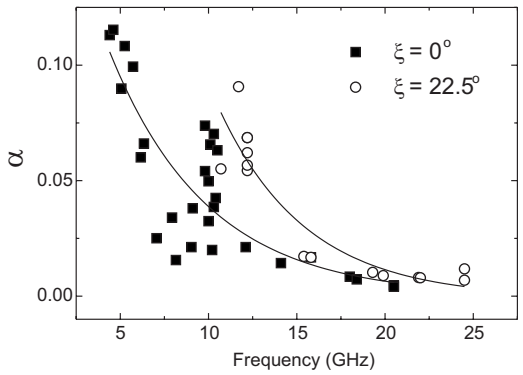

FIG. 8. Frequency variation of the damping parameter α at two different orientations of the in-plane magnetic field as indicated. Solid lines serve as guides to the eyes.

displays a behavior analogous to $\Delta\psi$. From the quite reasonable agreement between the experimental data and our calculations with respect to the field and azimuthal dependencies of the oscillation amplitudes, we can draw the following conclusions: (i) the LLG equation alone does not describe the dynamics of the system properly, (ii) an initial deflection of $\mathbf{M}$ by the pump-light pulse must be taken into account, and (iii) the subsequent magnetization precession takes place around the equilibrium orientation of $\mathbf{H}_{eff}$. With these modifications, the long-time dynamics of the system can be consistently described within the LLG model.

B. Damping of the precessional modes

In order to identify mechanisms responsible for the damping of the magnetization precession, a dimensionless damping parameter $\alpha=1/(\omega\mu)$, where μ corresponds to an exponential decay time, has been extracted from the time profiles of the magneto-optical response. In Fig. 8, this phenomenological damping parameter is plotted as a function of the precessional frequency for two orientations of the in-plane magnetic field at $\xi=0°$ and $\xi=22.5°$. We find that the damping parameter increases nonlinearly from $\alpha\sim 0.01$ at higher frequencies (saturation region) up to $\alpha\sim 0.1$ at lower frequencies. Besides, as one can see from a comparison of the guide-to-the-eye lines (solid lines in Fig. 8), the magnetization precession is damped faster at $\xi=22.5°$ than at $\xi=0°$ as the frequency decreases. This finding points toward an anisotropic character of the damping process.

The nonlinear behavior of the damping parameter as function of frequency, its orientational dependence (Fig. 8), as well as the relatively large values at low frequencies point out the necessity to account for mechanisms beyond the intrinsic Gilbert damping. We believe that the anisotropic and nonlinear behavior of the damping parameter is due to extrinsic contributions associated with a two magnon-scattering mechanism at the interfaces.[39] This is in agreement with previous studies evidencing the important contribution of this mechanism in Cr/Fe/GaAs(100) thin films.[20,21,29] In order to evaluate details of this mechanism, however, further experiments will be required.

VI. CONCLUSIONS

Using an all-optical pump-probe approach, we observed

that ultrashort optical pulses can induce long-living magnetization oscillations in Cr/Fe(100) thin films due to a thermal mechanism of the excitation. The in-plane fourfold anisotropy of the films is clearly reflected in their dynamical response. The magnetic-field and angular variations of the resonance frequency of the oscillations are well described by a general formalism used for FMR based on the Landau-Lifshitz-Gilbert equation. This behavior suggests that the main contribution to the observed behavior originates from the uniform precession mode. We may speculate that the inclusion of higher-order modes may still improve the agreement between experiment and model calculation. The amplitude of the excited oscillations essentially depends on the magnitude and orientation of the in-plane magnetic field relative to the crystallographic axes. The maximum efficiency of the excitation is realized at a magnetic field of 0.5 kOe, which is slightly deflected from the hard axis by about 4°. The excitation of the magnetization precession is associated with an initial transient deflection of the effective field away from the equilibrium orientation due to a local demagnetization of the sample (ΔM) and a change of the anisotropy constant (ΔK_1). This initial deflection marks the transition from the ultrafast dynamics to the precession-dominated (LLG) dynamical regime.

ACKNOWLEDGMENTS

The authors would like to thank R. Schreiber for the sample preparation. For B.B.K., this work was partially supported by RFFI project (No. 05-02-16451-a).

[1] S. A. Wolf, D. D. Awschalom, R. A. Buhrman, J. M. Daughton, S. von Molnar, M. L. Roukes, A. Y. Chtchelkanova, and D. M. Treger, Science **294**, 1488 (2001).
[2] G. A. Prinz, Science **282**, 1660 (1998).
[3] E. Beaurepaire, J.-C. Merle, A. Daunois, and J.-Y. Bigot, Phys. Rev. Lett. **76**, 4250 (1996).
[4] E. Beaurepaire, M. Maret, V. Halté, J.-C. Merle, A. Daunois, and J.-Y. Bigot, Phys. Rev. B **58**, 12134 (1998).
[5] G. P. Zhang and W. Hübner, Phys. Rev. Lett. **85**, 3025 (2000).
[6] H. Regensburger, R. Vollmer, and J. Kirschner, Phys. Rev. B **61**, 14716 (2000).
[7] B. Koopmans, M. van Kampen, J. T. Kohlhepp, and W. J. M. de Jonge, Phys. Rev. Lett. **85**, 844 (2000).
[8] L. Guidoni, E. Beaurepaire, and J.-Y. Bigot, Phys. Rev. Lett. **89**, 017401 (2002).
[9] P. M. Oppeneer and A. Liebsch, J. Phys.: Condens. Matter **16**, 5519 (2004).
[10] M. van Kampen, C. Jozsa, J. T. Kohlhepp, P. LeClair, L. Lagae, W. J. M. de Jonge, and B. Koopmans, Phys. Rev. Lett. **88**, 227201 (2002).
[11] R. Wilks, R. J. Hicken, M. Ali, B. J. Hickey, J. D. R. Buchanan, A. T. G. Pym, and B. K. Tanner, J. Appl. Phys. **95**, 7441 (2004).
[12] M. Vomir, L. H. F. Andrade, L. Guidoni, E. Beaurepaire, and J.-Y. Bigot, Phys. Rev. Lett. **94**, 237601 (2005); M. Vomir, L. H. F. Andrade, E. Beaurepaire, M. Albrecht, and J.-Y. Bigot, J. Appl. Phys. **99**, 08A501 (2006).
[13] C. D. Stanciu, A. V. Kimel, F. Hansteen, A. Tsukamoto, A. Itoh, A. Kiriliyuk, and Th. Rasing, Phys. Rev. B **73**, 220402(R) (2006).
[14] M. Djordjevic, M. Lüttich, P. Moschkau, P. Guderian, T. Kampfrath, R. G. Ulbrich, M. Münzenberg, W. Felsch, and J. S. Moodera, Phys. Status Solidi C **3**, 1347 (2006).
[15] A. Melnikov, I. Radu, U. Bovensiepen, O. Krupin, K. Starke, E. Matthias, and M. Wolf, Phys. Rev. Lett. **91**, 227403 (2003).
[16] M. Djordjevic, G. Eilers, A. Parge, M. Münzenberg, and J. S. Moodera, J. Appl. Phys. **99**, 08F308 (2006).
[17] G. Ju, A. V. Nurmikko, R. F. C. Farrow, R. F. Marks, M. J. Carey, and B. A. Gurney, Phys. Rev. Lett. **82**, 3705 (1999); G. Ju, L. Chen, A. V. Nurmikko, R. F. C. Farrow, R. F. Marks, M. J. Carey, and B. A. Gurney, Phys. Rev. B **62**, 1171 (2000).
[18] M. C. Weber, H. Nembach, and J. Fassbender, J. Appl. Phys. **95**, 6613 (2004); M. C. Weber, H. Nembach, and B. Hillebrands, *ibid.* **97**, 10A701 (2005).
[19] F. Dalla Longa, J. T. Kohlhepp, W. J. M. de Jonge, and B. Koopmans, J. Appl. Phys. **99**, 08F304 (2006).
[20] R. Urban, B. Heinrich, G. Woltersdorf, K. Ajdari, K. Myrtle, J. F. Cochran, and E. Rozenberg, Phys. Rev. B **65**, 020402(R) (2001).
[21] B. K. Kunar, R. E. Camley, and Z. Celinski, J. Appl. Phys. **95**, 6610 (2004).
[22] T. Martin, B. Becker, S. Ganzer, T. Hagler, M. Sperl, and G. Bayreuther, J. Appl. Phys. **97**, 10A718 (2005).
[23] D. M. Engebretson, J. Berezovsky, J. P. Park, L. C. Chen, C. J. Palmstrom, and P. A. Crowell, J. Appl. Phys. **91**, 8040 (2002).
[24] T. J. Silva, C. S. Lee, T. M. Crawford, and C. T. Rogers, J. Appl. Phys. **85**, 7849 (1999).
[25] R. J. Hicken, A. Ercole, S. J. Gray, C. Daboo, and J. A. C. Bland, J. Appl. Phys. **79**, 4987 (1996).
[26] R. J. Hicken, S. J. Gray, A. Ercole, C. Daboo, D. J. Freeland, E. Gu, E. Ahmad, and J. A. C. Bland, Phys. Rev. B **55**, 5898 (1997).
[27] M. G. Pini, P. Politi, A. Rettori, G. Carlotti, G. Gubbiotti, M. Madami, and S. Tacchi, Phys. Rev. B **70**, 094422 (2004).
[28] M. Madami, S. Tacchi, G. Carlotti, G. Gubbiotti, and R. L. Stamps, Phys. Rev. B **69**, 144408 (2004).
[29] G. Woltersdorf, M. Buess, B. Heinrich, and C. H. Back, Phys. Rev. Lett. **95**, 037401 (2005).
[30] M. Buess, T. P. J. Knowles, U. Ramsperger, D. Pescia, and C. H. Back, Phys. Rev. B **69**, 174422 (2004).
[31] F. Hansteen, A. V. Kimel, A. Kirilyuk, and Th. Rasing, Phys. Rev. Lett. **95**, 047402 (2005).
[32] G. V. Astakhov, A. V. Kimel, G. M. Schott, A. A. Tsvetkov, A. Kirilyuk, D. R. Yakovlev, G. Karczewski, W. Ossau, G. Schmidt, L. W. Molenkamp, and Th. Rasing, Appl. Phys. Lett. **86**, 152506 (2005).
[33] D. E. Bürgler, C. M. Schmidt, D. M. Schaller, F. Meisinger, R. Hofer, and H.-J. Güntherodt, Phys. Rev. B **56**, 4149 (1997).
[34] B. Heinrich and J. F. Cochran, Adv. Phys. **42**, 523 (1993).
[35] A. K. Zvezdin and V. A. Kotov, *Modern Magnetooptics and*

Magnetooptical Materials (IOP, Bristol, 1997).
[36] R. M. Osgood III, B. M. Clemens, and R. L. White, Phys. Rev. B **55**, 8990 (1997).
[37] J. Smit and H. G. Beljers, Philips Res. Rep. **10**, 113 (1955).
[38] B. Koopmans, in *Spin Dynamics in Confined Magnetic Structures II*, Topics in Applied Physics Vol. 87, edited by B. Hillebrands and K. Ounadjela (Springer, Berlin, 2002), p. 253.
[39] R. Arias and D. L. Mills, Phys. Rev. B **60**, 7395 (1999).